

# Proton Form Factor

PRL **105**, 242001 (2010)

PHYSICAL REVIEW LETTERS

week ending  
10 DECEMBER 2010



## High-Precision Determination of the Electric and Magnetic Form Factors of the Proton

J. C. Bernauer,<sup>1,\*</sup> P. Achenbach,<sup>1</sup> C. Ayerbe Gayoso,<sup>1</sup> R. Böhm,<sup>1</sup> D. Bosnar,<sup>2</sup> L. Debenjak,<sup>3</sup> M. O. Distler,<sup>1,†</sup> L. Doria,<sup>1</sup> A. Esser,<sup>1</sup> H. Fonvieille,<sup>4</sup> J. M. Friedrich,<sup>5</sup> J. Friedrich,<sup>1</sup> M. Gómez Rodríguez de la Paz,<sup>1</sup> M. Makek,<sup>2</sup> H. Merkel,<sup>1</sup> D. G. Middleton,<sup>1</sup> U. Müller,<sup>1</sup> L. Nungesser,<sup>1</sup> J. Pochodzalla,<sup>1</sup> M. Potokar,<sup>3</sup> S. Sánchez Majos,<sup>1</sup> B. S. Schlimme,<sup>1</sup> S. Širca,<sup>6,3</sup> Th. Walcher,<sup>1</sup> and M. Weinriefer<sup>1</sup>

(A1 Collaboration)

<https://journals.aps.org/prl/abstract/10.1103/PhysRevLett.105.242001>

## Electric and magnetic form factors of the proton

J. C. Bernauer, M. O. Distler, J. Friedrich, Th. Walcher, P. Achenbach, C. Ayerbe Gayoso, R. Böhm, D. Bosnar, L. Debenjak, L. Doria, A. Esser, H. Fonvieille, M. Gómez Rodríguez de la Paz, J. M. Friedrich, M. Makek, H. Merkel, D. G. Middleton, U. Müller, L. Nungesser, J. Pochodzalla, M. Potokar, S. Sánchez Majos, B. S. Schlimme, S. Širca, and M. Weinriefer (A1 Collaboration)

Phys. Rev. C **90**, 015206 – Published 29 July 2014

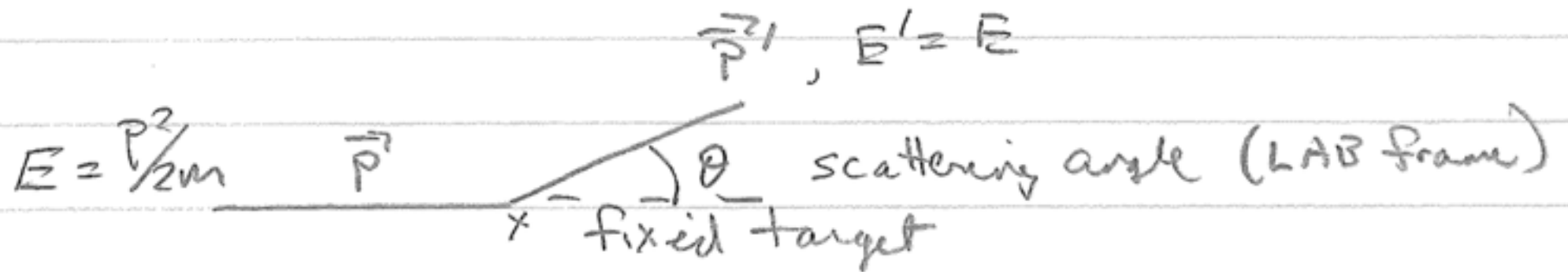
<https://arxiv.org/pdf/1307.6227.pdf>

# Rutherford Scattering

Recall Rutherford (phy 450, lec 2)

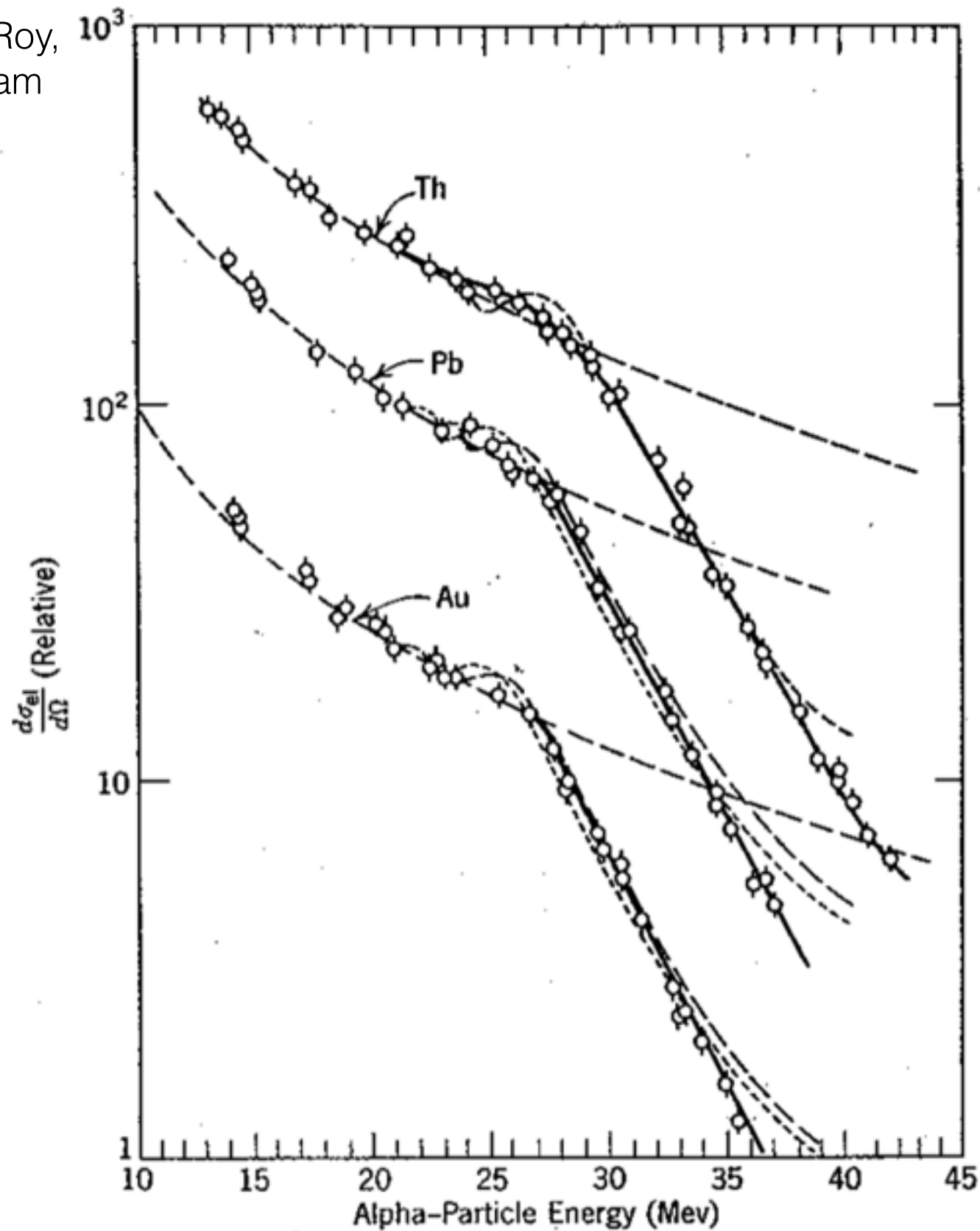
Coulomb potential  $1/r$

$$\frac{d\sigma^R}{d\Omega} = \frac{1}{(4\pi)^2} \frac{(ZZ'e\hbar c\alpha)^2}{\sin^4(\theta/2)} \quad \text{classical and quantum cross sections are identical}$$



3 - momentum transfer  $\vec{q} = |\vec{p}' - \vec{p}| = 2p^2(1 - \cos\theta)$   
 $= 4p^2 \sin^2(\theta/2)$

Friday

from Roy,  
Nigam

Alpha-Particle Energy (Mev)

Fig. 2-1 The broad dashed curve gives the Coulomb cross section, and the solid curve represents the experimental data of Farwell and Wegner<sup>4</sup> for Au, Pb, and Th. For Au, the finer theoretical curve corresponds to  $R = 10.58 \times 10^{-13}$  cm and the coarser curve to  $R = 10.3 \times 10^{-13}$  cm. For Pb, the finer curve corresponds to  $R = 10.87 \times 10^{-13}$  cm and the coarser to  $R = 10.42 \times 10^{-13}$  cm. For Th, the dashed curve corresponds to  $R = 11.01 \times 10^{-13}$  cm (Eisberg and Porter<sup>1</sup>).

# Mott Scattering

Mott cross section

relativistic  $v/c \approx 1$

$e^-$  elastic

$$\frac{d\sigma^{\text{Mott}}}{d\Omega} = \underbrace{\frac{(Z\alpha\hbar c)^2}{4E_0^2 \sin^4 \frac{\theta}{2}}}_{\text{Rutherford}} \underbrace{\left(\frac{E}{E_0}\right)}_{\text{recoil}} \underbrace{\cos^2 \frac{\theta}{2}}_{\text{spin}}$$

Spin:

incoming plane wave has  $L_z = 0$ .

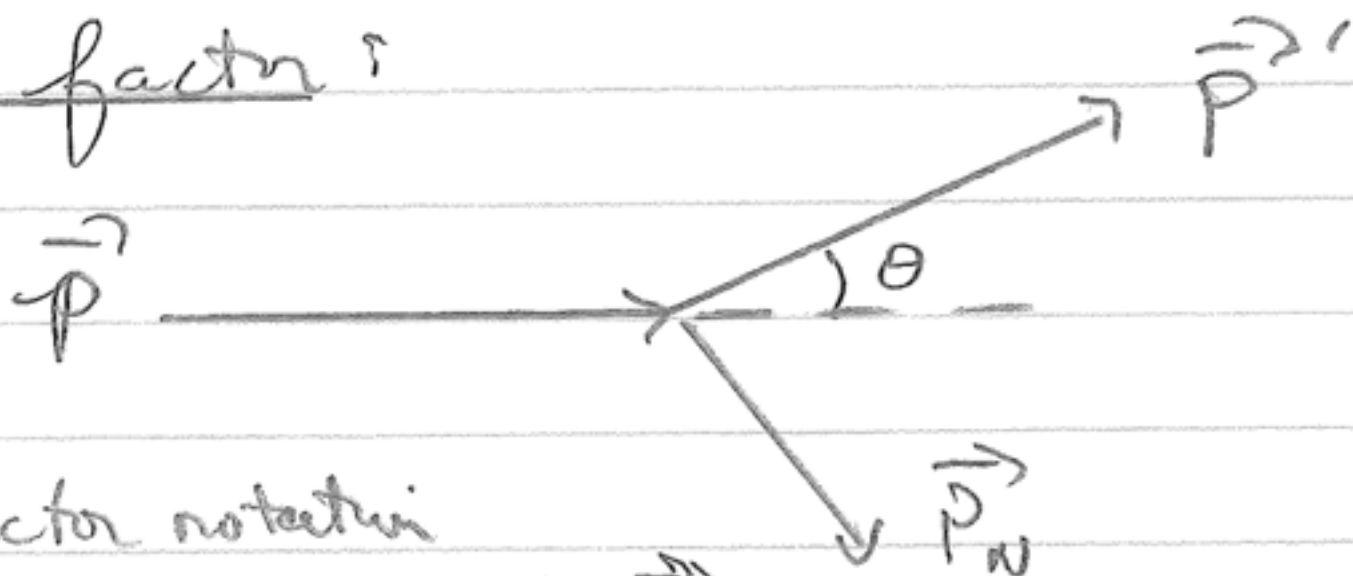
Assuming interaction does not flip spin  
(true for Coulomb interaction):



Spin

$$\text{Amplitude} = \langle \frac{1}{2}, \pm \frac{1}{2} | \frac{1}{2}, \pm \frac{1}{2} \rangle_{p'} = \cos^2 \frac{\theta}{2}$$

recoil factor ?



in 4-vector notation

$$\vec{P} \equiv (E, \vec{P}) \longrightarrow (P, \vec{P})$$

ultra-relativistic. ( $c \equiv 1$  units)

$$\vec{P} = E_0 (1, \hat{z})$$

$$\vec{P}' = E (1, \hat{r})$$

$$4\text{-momentum transfer } -q^2 = -(\vec{P} - \vec{P}')^2$$

$$-g^2 = -(\vec{P} - \vec{P}')^2 = 2E_0 E (1 - \cos\theta) = 4E_0 E \sin^2 \theta/2$$

E-conservation determines E( $\theta$ )

$$E_0 + m_N = E + E_N \quad (\text{LAB frame})$$

$$\begin{aligned} (E_0 + m_N - E)^2 &= E_N^2 = m_N^2 + |\vec{P}_N|^2 \\ &= m_N^2 + |\vec{P} - \vec{P}'|^2 \end{aligned}$$

$$\begin{aligned} &= m_N^2 + E_0^2 + E^2 - 2E_0 E \cos\theta \\ &= m_N^2 + (E_0 - E)^2 + 4E_0 E \sin^2 \theta/2 \end{aligned}$$

$$\text{then } (E_0 - E)^2 + 2m_N (E_0 - E) + m_N^2$$

$$= m_N^2 + (E_0 - E)^2 + 4E_0 E \sin^2 \theta/2$$

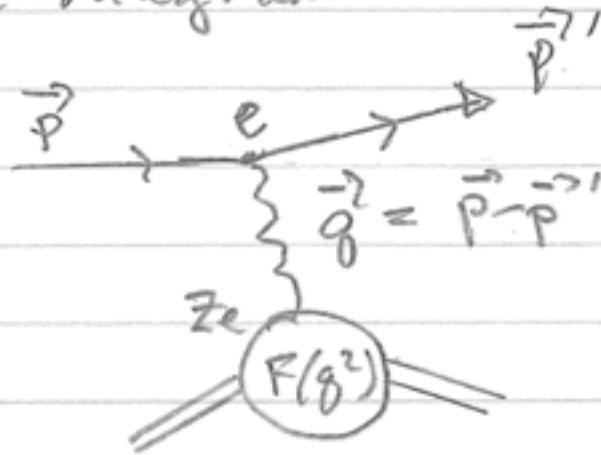
$$\left( \frac{1}{E} - \frac{1}{E_0} \right)^2 = \frac{2 \sin^2 \theta/2}{m_N}$$

$$\text{factor } \frac{E}{E_0} = \left( 1 + \frac{2E_0 \sin^2 \theta/2}{m_N} \right)^{-1}$$

# Form Factor

## Nuclear form factor

Feynman diagram



$F(q^2)$  takes into account non-pointlike nucleus

$$F(q^2) = \int \rho(\vec{R}) e^{i\vec{q}\cdot\vec{R}} d^3R$$

↑  
nuclear charge density

$$\frac{d\sigma}{d\Omega} = \frac{d\sigma}{d\Omega}^{\text{Mott}} |F(q^2)|^2$$

Approximation

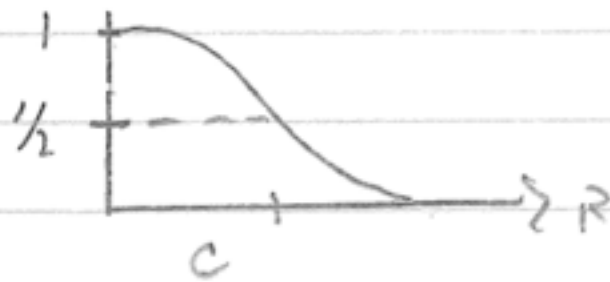
"dipole"  $f(R) = f_0 e^{-R/a}$

$$F(g^2) = [1 + (gR)^2]^{-1}$$

better

$$f(R) = f_0 \left[ 1 + e^{-(r-c)/a} \right]^{-1}$$

$f(R)/f_0$



- Nuclei are not spheres with a sharply defined surface. In their interior, the charge density is nearly constant. At the surface the charge density falls off over a relatively large range. The radial charge distribution can be described to good approximation by a Fermi function with two parameters

$$\rho(r) = \frac{\rho(0)}{1 + e^{(r-c)/a}} \quad (5.52)$$

This is shown in Fig. 5.8 for different nuclei.

- The constant  $c$  is the radius at which  $\rho(r)$  has decreased by one half. Empirically, for larger nuclei,  $c$  and  $a$  are measured to be:

$$c = 1.07 \text{ fm} \cdot A^{1/3}, \quad a = 0.54 \text{ fm}. \quad (5.53)$$

- From this charge density, the mean square radius can be calculated. Approximately, for medium and heavy nuclei:

$$\langle r^2 \rangle^{1/2} = r_0 \cdot A^{1/3} \quad \text{where } r_0 = 0.94 \text{ fm}. \quad (5.54)$$

The nucleus is often approximated by a homogeneously charged sphere. The radius  $R$  of this sphere is then quoted as the nuclear radius. The following connection exists between this radius and the mean square radius:

$$R^2 = \frac{5}{3} \langle r^2 \rangle. \quad (5.55)$$

Quantitatively we have:

$$R = 1.21 \cdot A^{1/3} \text{ fm}. \quad (5.56)$$

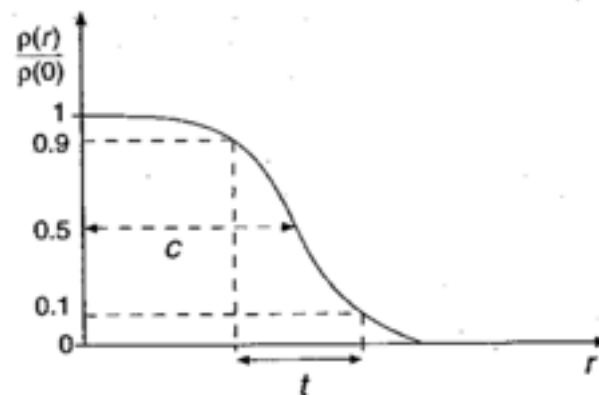
This definition of the radius is used in the mass formula (2.8).

- The surface thickness  $t$  is defined as the thickness of the layer over which the charge density drops from 90% to 10% of its maximal value:

$$t = r_{(\rho/\rho_0=0.1)} - r_{(\rho/\rho_0=0.9)}. \quad (5.57)$$

Its value is roughly the same for all heavy nuclei, namely:

$$t = 2a \cdot \ln 9 \approx 2.40 \text{ fm}. \quad (5.58)$$



from Rovh, Rith,  
Scholz, Zetsche

$$\left(\frac{d\sigma}{d\Omega}\right) = \left(\frac{d\sigma}{d\Omega}\right)_{\text{Mott}} \frac{\varepsilon G_E^2 + \tau G_M^2}{\varepsilon(1 + \tau)}, \quad (1)$$

where  $G_E$  and  $G_M$  are the electric and magnetic Sachs form factors,  $m_p$  is the proton mass,  $\tau = Q^2/(4m_p^2c^2)$  and  $\varepsilon = [1 + 2(1 + \tau)\tan^2(\theta/2)]^{-1}$  with the electron scattering angle  $\theta$ . However, also electromagnetic processes of higher order contribute to the measured cross section, such as multiple photon exchange, vacuum polarization, vertex corrections, and the radiation of a real photon from the electron (Bethe-Heitler) or the proton (Born).

The code simulating the cross-section integration over the acceptance includes these processes following the description of Ref. [8] which gives results compatible with Ref. [9]. Our approach extends this by an explicit calculation of the Feynman graphs of the Bethe-Heitler and Born processes on the event level. The simulation uses the standard dipole parametrization

$$G_E = \frac{G_M}{\mu_p} = G_{\text{std.dip.}} = \left(1 + \frac{Q^2}{0.71 (\text{GeV}/c)^2}\right)^{-2} \quad (2)$$

as a sufficient approximation for the true form factors ( $\mu_p$  is the proton's magnetic moment divided by the nuclear magneton). The division of the measured number of elas-

# updated experiment/analysis

<https://arxiv.org/pdf/1307.6227.pdf>

Mainz Microtron (MAMI): 20  $\mu$ A

<http://www.kph.uni-mainz.de/eng/108.php>

Department of Physics, University of Virginia, Charlottesville.  
(Dated: July 30, 2014)

This paper describes a precise measurement of electron scattering off the proton at momentum transfers of  $0.003 \lesssim Q^2 \lesssim 1 \text{ GeV}^2$ . The average point-to-point error of the cross sections in this experiment is  $\sim 0.37\%$ . These data are used for a coherent new analysis together with all world data of unpolarized and polarized electron scattering from the very smallest to the highest momentum transfers so far measured. The extracted electric and magnetic form factors provide new insight into their exact shape, deviating from the classical dipole form, and of structure on top of this gross shape. The data reaching very low  $Q^2$  values are used for a new determination of the electric and magnetic radii. An empirical determination of the two-photon-exchange correction is presented. The implications of this correction on the radii and the question of a directly visible signal of the pion cloud are addressed.

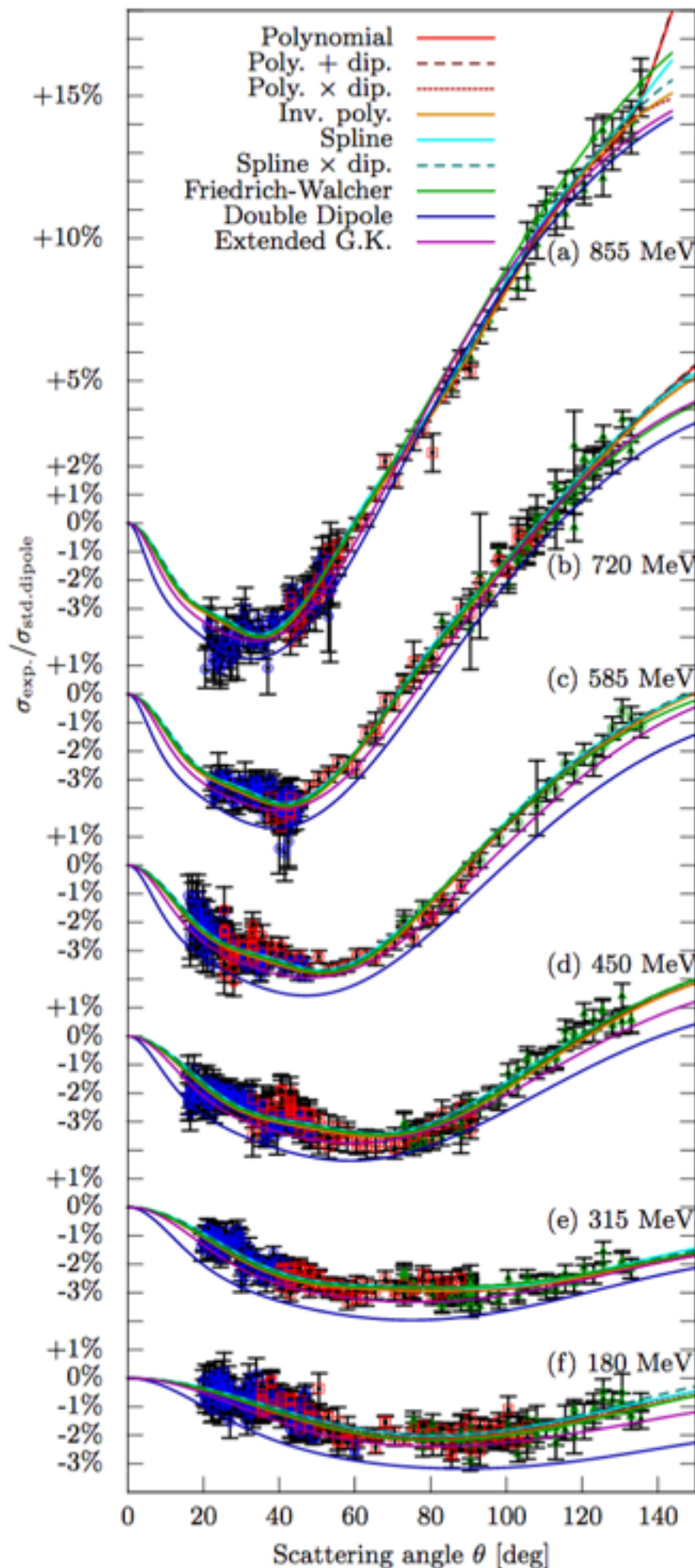


FIG. 9. (Color) The cross sections and the fits for 855, 720, 585, 450, 315 and 180 MeV [(a)-(f)] incident beam energy divided by the cross section calculated with the standard dipole, as functions of the scattering angle (red: measured with spectrometer A; blue: spectrometer B; green: spectrometer C). The normalization parameters  $n_j$  applied to the measured cross section data are taken from the spline fit. The cross sections of the fits that achieve a good  $\chi^2 < 1600$  differ by at most 0.7%. The normalization parameters  $n_j$  from the double-dipole fit would shift the data down by 1.6% at most. Accordingly, its curve lies below the data with the normalizations from the spline fit.

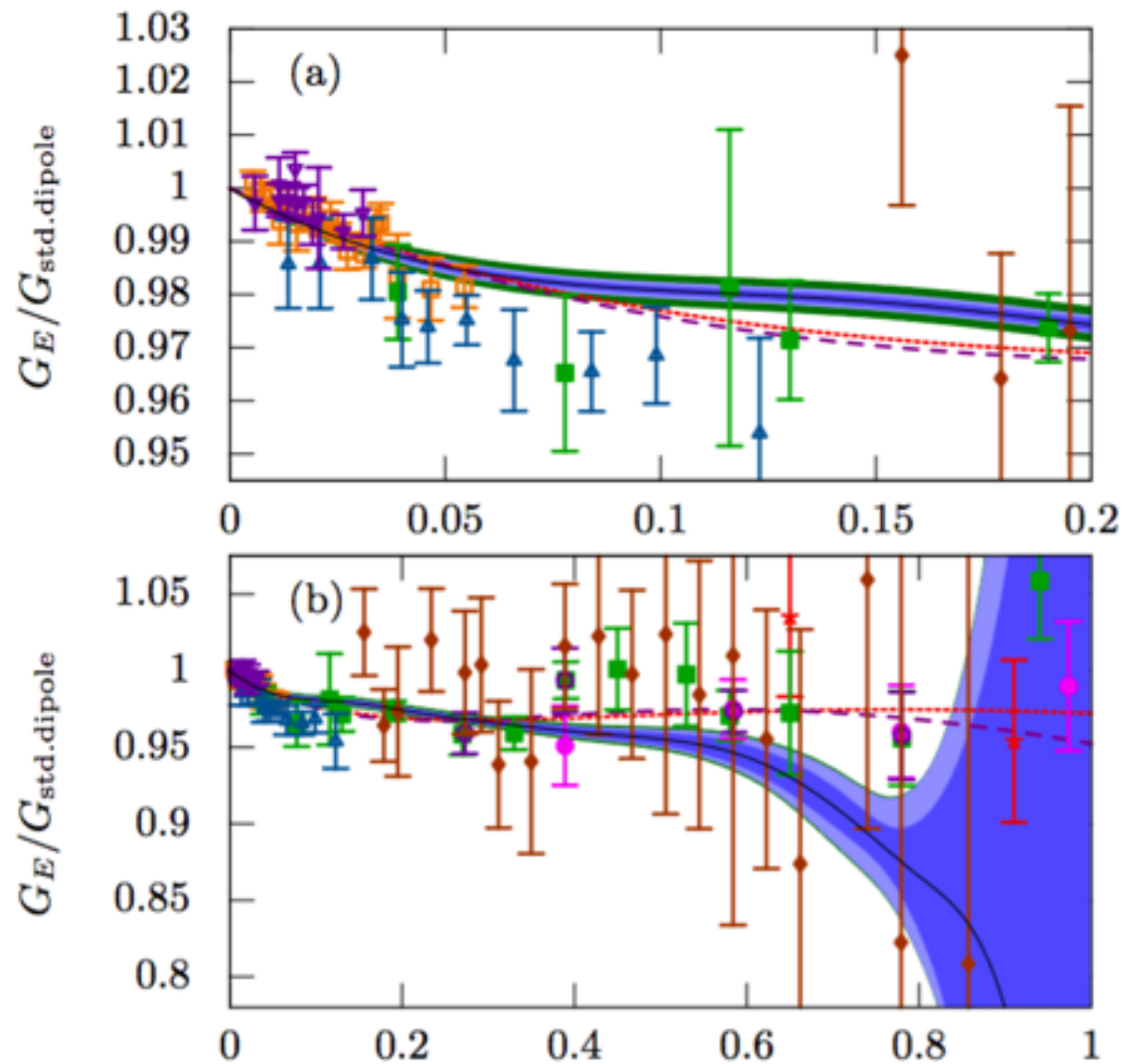
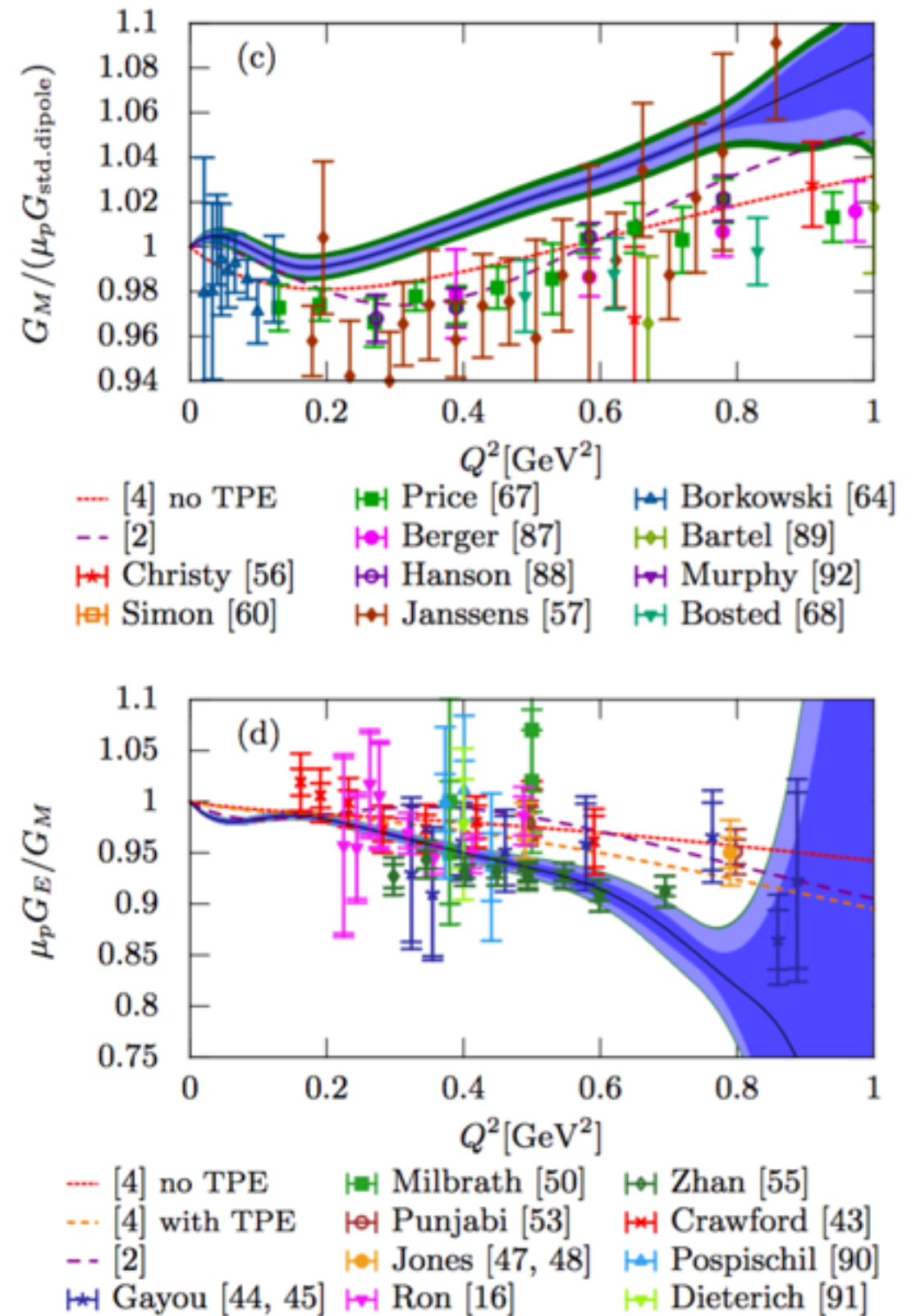


FIG. 10. (Color) The form factors  $G_E$  and  $G_M$ , normalized to the standard dipole, and  $G_E/G_M$  as a function of  $Q^2$ . Black line: Best fit to the new Mainz data, blue area: statistical 68% pointwise confidence band, light blue area: experimental systematic error, green outer band: variation of the Coulomb correction by  $\pm 50\%$ . The different data points depict the previous measurements [2, 4, 43–45, 47, 48, 50, 53, 55–57, 60, 67, 68, 87–91] as in Refs. [2, 4] with the data points of Refs. [16, 64, 92] added.



The structure at small  $Q^2$  seen in both form factors corresponds to the scale of the pion of about  $Q^2 \approx m_\pi^2 \approx 0.02 \text{ (GeV}/c)^2$  and may be indicative of the influence of the pion cloud [1].

[1] for further discussion of pion cloud

<https://arxiv.org/pdf/1008.4225.pdf>

experiment.

The charge and magnetic rms radii are given by

$$\langle r_{E/M}^2 \rangle = - \frac{6\hbar^2}{G_{E/M}(0)} \left. \frac{dG_{E/M}(Q^2)}{dQ^2} \right|_{Q^2=0}. \quad (3)$$

In the study of the model dependency through simulated data only the flexible models reproduce the input radii reliably. In the fits to the measured data the models can be divided into two groups: Those based on splines with varying degree of the basis polynomial and number of support points and those composed of polynomials with varying orders. For the charge radius the weighted averages of the two groups differ by 0.008 fm.

For the spline group we obtain the values

$$\begin{aligned} \langle r_E^2 \rangle^{1/2} &= 0.875(5)_{\text{stat}}(4)_{\text{syst}}(2)_{\text{model}} \text{ fm}, \\ \langle r_M^2 \rangle^{1/2} &= 0.775(12)_{\text{stat}}(9)_{\text{syst}}(4)_{\text{model}} \text{ fm} \end{aligned} \quad (4)$$

and for the polynomial group

$$\begin{aligned} \langle r_E^2 \rangle^{1/2} &= 0.883(5)_{\text{stat}}(5)_{\text{syst}}(3)_{\text{model}} \text{ fm}, \\ \langle r_M^2 \rangle^{1/2} &= 0.778 \begin{pmatrix} +14 \\ -15 \end{pmatrix}_{\text{stat}} (10)_{\text{syst}}(6)_{\text{model}} \text{ fm}. \end{aligned} \quad (5)$$

Despite detailed studies the cause of the difference between the two model groups could not be found. Therefore, we give as the final result the average of the two values with an additional uncertainty of half of the difference

$$\begin{aligned} \langle r_E^2 \rangle^{1/2} &= 0.879(5)_{\text{stat}}(4)_{\text{syst}}(2)_{\text{model}}(4)_{\text{group}} \text{ fm}, \\ \langle r_M^2 \rangle^{1/2} &= 0.777(13)_{\text{stat}}(9)_{\text{syst}}(5)_{\text{model}}(2)_{\text{group}} \text{ fm}. \end{aligned}$$

Method	Electric radius $r_E$ in fm
Spline models (1)	$0.875(5)_{\text{stat.}}(4)_{\text{syst.}}(2)_{\text{model}}$
Polynomial models (2)	$0.883(5)_{\text{stat.}}(5)_{\text{syst.}}(3)_{\text{model}}$
Friedrich-Walcher	$0.884(_{-8}^{+7})_{\text{stat.}}(_{-5}^{+7})_{\text{syst.}}$
Spline with variable knots + external data:	
+ Rosenbluth data	0.878
+ all external data	0.878
<b>Average of (1),(2)</b>	$0.879(5)_{\text{stat.}}(4)_{\text{syst.}}(2)_{\text{model}}(4)_{\text{group}}$
With TPE from [96]	$0.876(5)_{\text{stat.}}(4)_{\text{syst.}}(2)_{\text{model}}(5)_{\text{group}}$
With TPE from [97–99]	$0.875(5)_{\text{stat.}}(4)_{\text{syst.}}(2)_{\text{model}}(5)_{\text{group}}$

TABLE X. Results for the electric radius.

still conflicts with muonic  
Lamb shift

“TPE” from Hydrogen  
hyperfine

Method	Magnetic radius $r_M$ in fm
Spline models (1)	$0.775(12)_{\text{stat.}}(9)_{\text{syst.}}(4)_{\text{model}}$
Polynomial models (2)	$0.778(_{-15}^{+14})_{\text{stat.}}(10)_{\text{syst.}}(6)_{\text{model}}$
Friedrich-Walcher	$0.807(2)_{\text{stat.}}(_{-1}^{+4})_{\text{syst.}}$
Spline with variable knots + external data:	
+ Rosenbluth data	0.772
+ all external data	0.769
<b>Average of (1),(2)</b>	$0.777(13)_{\text{stat.}}(9)_{\text{syst.}}(5)_{\text{model}}(2)_{\text{group}}$
With TPE from [96]	$0.803(13)_{\text{stat.}}(9)_{\text{syst.}}(5)_{\text{model}}(3)_{\text{group}}$
With TPE from [97–99]	$0.799(13)_{\text{stat.}}(9)_{\text{syst.}}(5)_{\text{model}}(3)_{\text{group}}$

TABLE XI. Results for the magnetic radius.

calculation may affect the results slightly.

The electric radius is in complete agreement with the CODATA06 [20] value of 0.8768(69) fm based mostly on atomic measurements. It is also in complete accord with the old Mainz result [21] when the Coulomb corrections [5,6] are applied. However, the results from very recent Lamb shift measurements on muonic hydrogen [22] are 0.04 fm smaller, i.e., 5 standard deviations. This difference

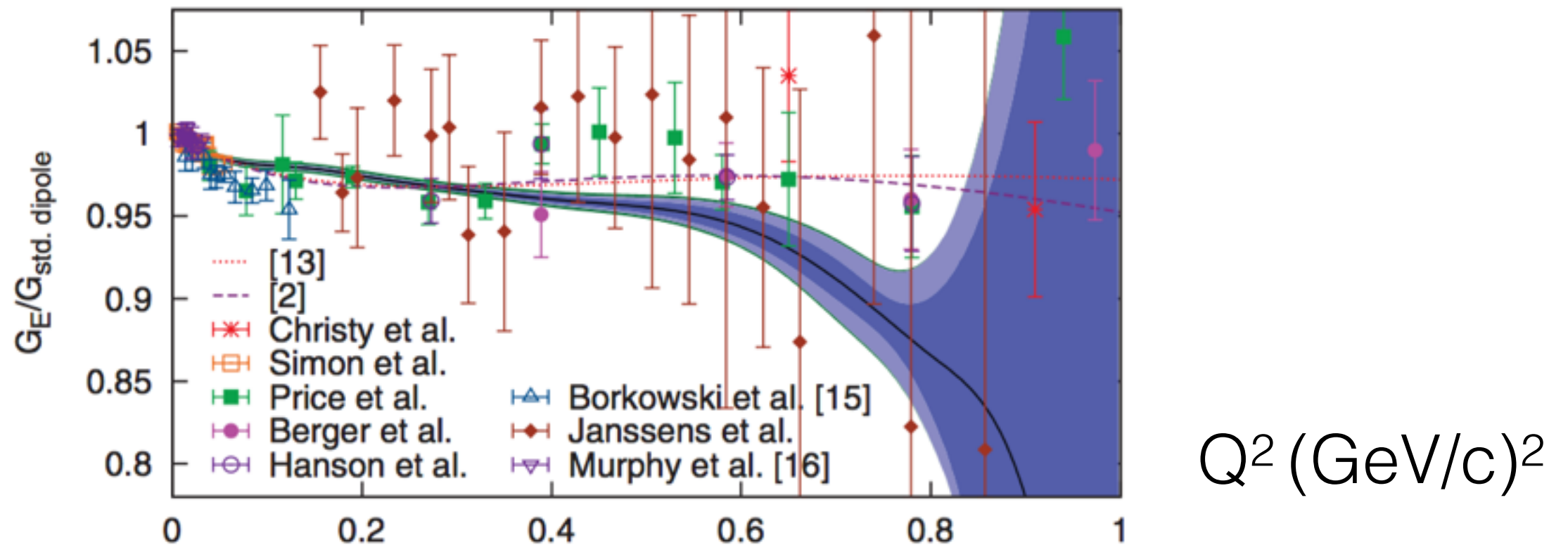
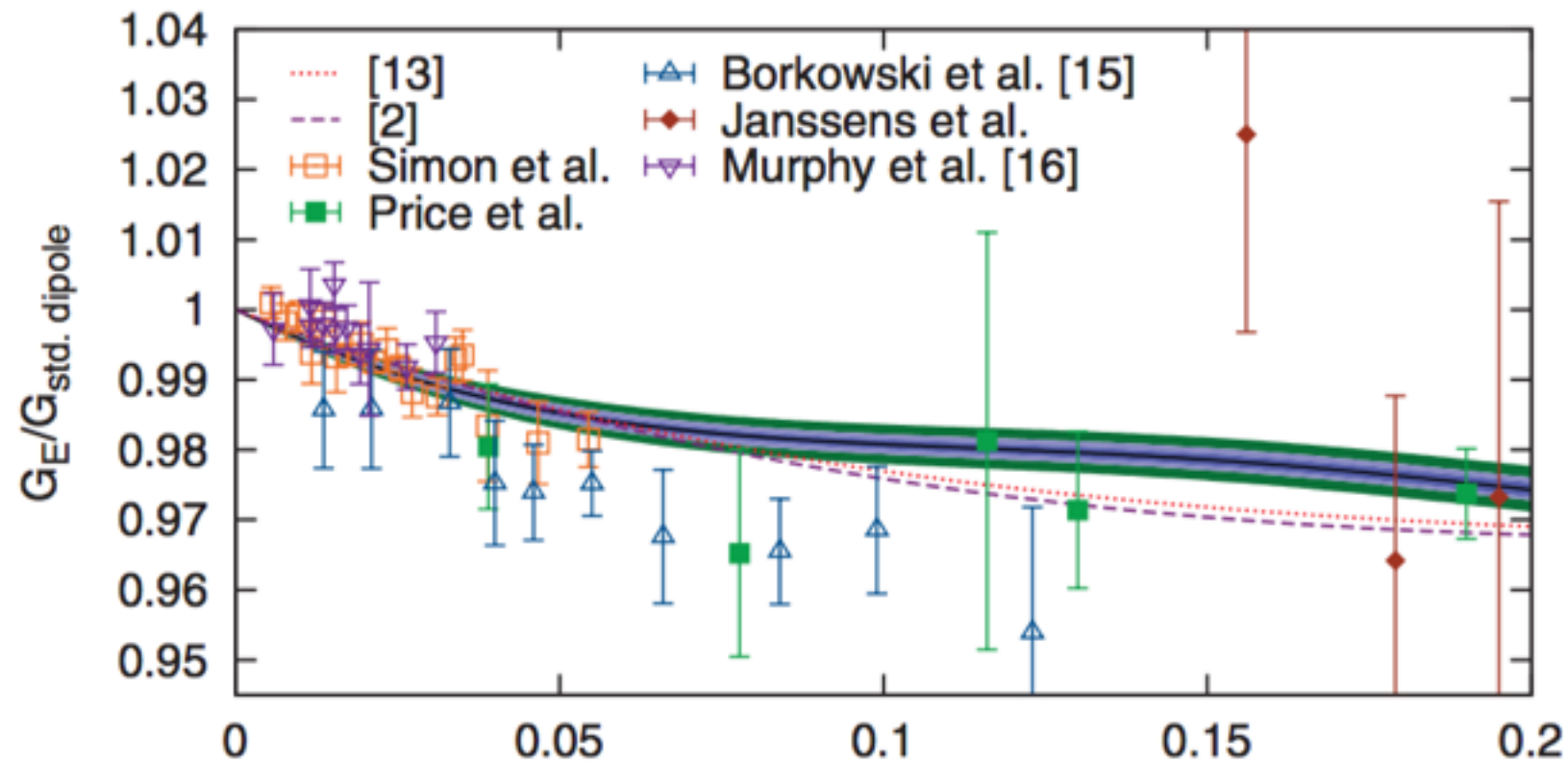
is unexplained yet. The calculation of the Lamb shift in muonic hydrogen requires the solution of a relativistic bound state problem (see Ref. [23] and references therein). The deviation may be due to the distorted wave functions, significantly more distorted than in electronic hydrogen, necessitating the consideration of multiphoton exchange.

The magnetic radius has a larger error than the charge radius since the experiment is less sensitive to  $G_M$  at low  $Q^2$ . Its value is smaller than results of previous fits, however, it is in good agreement with Ref. [24], who found 0.778(29) fm from hyperfine splitting in hydrogen.

The consequences of the results presented here for our picture of the proton are discussed in Ref. [1]. A full account of this work will be published [25,26].

## 2010 Fits

About 1400 cross sections were measured at beam energies of 180, 315, 450, 585, 720, and 855 MeV covering  $Q^2$  from 0.004 to 1  $(\text{GeV}/c)^2$



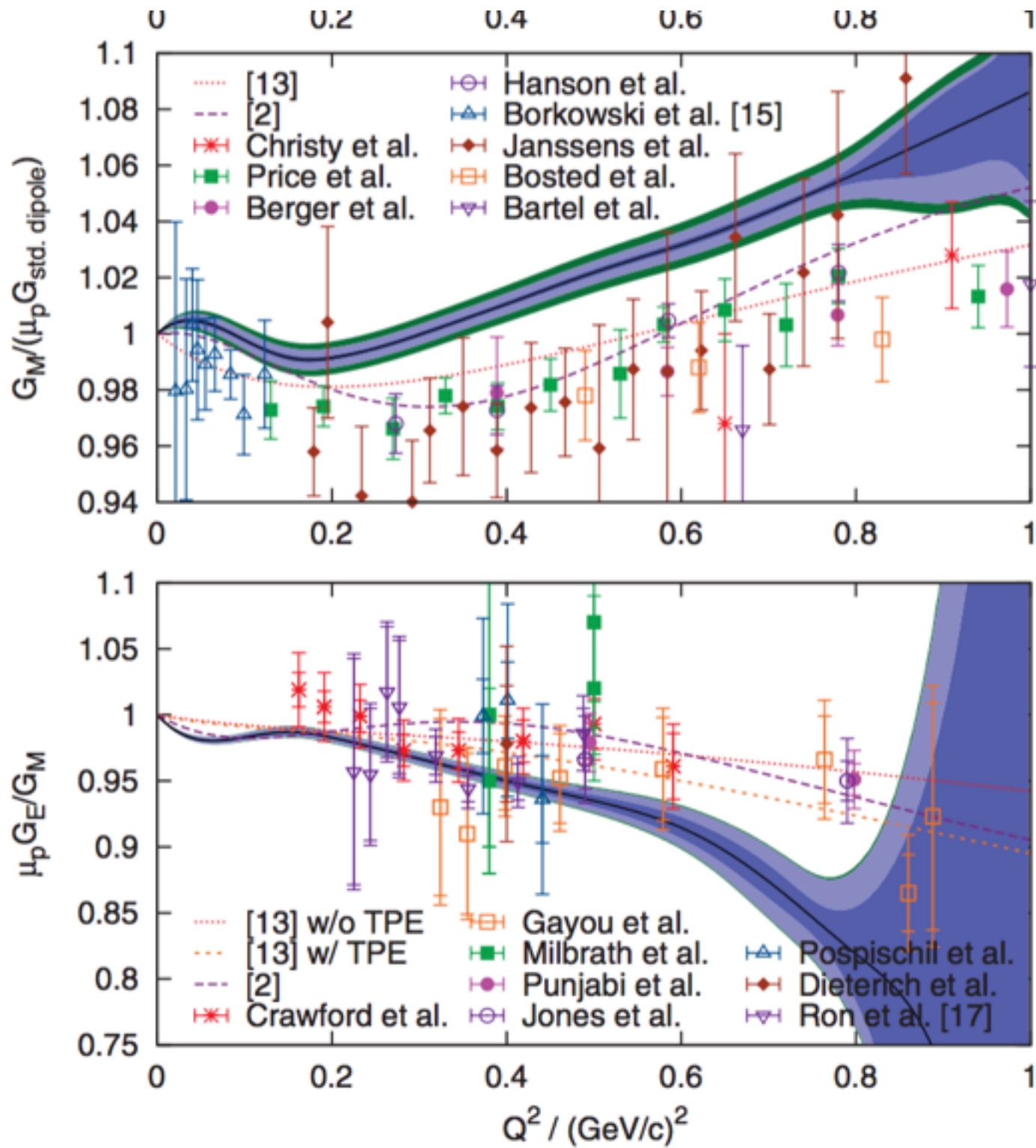


FIG. 2 (color). The form factors  $G_E$  and  $G_M$  normalized to the standard dipole and  $G_E/G_M$  as a function of  $Q^2$ . Black line: best fit to the data, blue area: statistical 68% pointwise confidence band, light blue area: experimental systematic error, green outer band: variation of the Coulomb correction by  $\pm 50\%$ . The different data points depict previous measurements, for Refs. see [2,13]; we added the data points of [15–17]. Dashed lines are previous fits to the old data in [2,13].